Intensive Care Med (2012) 38:1917–1929
DOI 10.1007/s00134-012-2684-z

REVIEW

Steffen Leonhardt
Burkhard Lachmann

Electrical impedance tomography: the holy grail of ventilation and perfusion monitoring?

Received: 27 July 2011
Accepted: 8 August 2012
Published online: 20 September 2012

Electronic supplementary material
The online version of this article (doi:10.1007/s00134-012-2684-z) contains supplementary material, which is available to authorized users.

S. Leonhardt (✉)
Philips Chair for Medical Information Technology, Helmholtz Institute, RWTH Aachen University, Aachen, Germany
e-mail: leonhardt@hia.rwth-aachen.de
Tel.: +49-241-8023211
Fax: +49-241-8082442

B. Lachmann
Department of Anaesthesiology, Charite Campus Virchow-Klinikum (CVK), Berlin, Germany
e-mail: Burkhard.lachmann@gmail.com

Abstract This review summarizes the state-of-the-art in electrical impedance tomography (EIT) for ventilation and perfusion imaging. EIT is a relatively new technology used to image regional impedance distributions in a cross-sectional area of the body. After the introduction, a brief overview of the recent history is provided followed by a review of the literature on regional ventilation monitoring using EIT. Several recently presented indices that are useful to extract information from EIT image streams are described. Selected experimental and clinical findings are discussed with respect to future routine applications in intensive care. Finally, past and ongoing research activities aimed at obtaining cardiac output and regional perfusion information from EIT image streams are summarized.

Keywords Electrical impedance tomography · EIT · Regional ventilation monitoring · Regional perfusion monitoring

Introduction

For many years, clinicians have been looking for a proper way to evaluate the quality of ventilatory assistance for the individual patient. While some parameters, e.g., (dynamic) respiratory compliance, lower inflection point, pressure–time relationships, are available, there has been growing awareness that such global parameters may not be sufficient, and that in order to prevent lung damage, we will need to monitor regional lung mechanics at the bedside. A technology suitable for this task seems to be electrical impedance tomography (EIT) [1], which has recently received increasing attention from the intensive care community [2–5].

EIT is a noninvasive, radiation-free, and real-time imaging modality which is easy to use, not harmful to the patient, and offers regional information about ventilation and possibly eventually perfusion not available with any other monitoring modality. This method relies on the visualization and quantification of tissue impedance determined by injecting small electrical currents and measuring the resulting voltages at the surface of the torso. Owing to its capability to show changes in tissue impedance very quickly, it may be a valuable tool to adjust ventilator settings for the individual patient at the bedside [6, 7].

The literature on EIT is expanding rapidly [8] and new commercial devices are becoming available. Therefore, an increasing use in the clinical setting can be forecasted.

This review intends to provide a basis for understanding this development by summarizing the state-of-the-art and presenting a methodology to classify older findings and recent research activities.

Basic principle of EIT

In biological tissues, the conduction of electrical current is based on the local amount of fluid and ion concentration. Considering the lung, we note that the electrical current cannot flow through the alveoli, but only around them through the alveolar septa. While an increase in alveolar volume stretches and prolongs the average current pathways increasing the overall electrical resistance, expiration reduces the overall tissue resistance due to shorter and thicker current pathways.

In EIT, the distribution of local tissue resistance (or, more generally, impedance) within a cross section of the body is displayed as a tomographic image. As impedance Z is defined as voltage V over current I, regional impedance may be computed from measurements of currents and corresponding voltages on the surface (Fig. 1).

At any time, there are an active pair of current-injecting electrodes and a separate pair of electrodes for voltage measurements. A typical setting is to inject a small alternating electrical current, e.g., 5 mA at a frequency of 50 kHz. To become independent of skin and electrode impedances, EIT expands the classical 4-electrode bioimpedance principle by continuously rotating the location of current injection and voltage measurements around the body on a plane, thus spanning a cross section. Typically, for lung monitoring the 4th–6th intercostal space is used.

In such a circumferential electrode arrangement, there are different ways to combine electrodes. The most popular configuration is referred to as "adjacent drive configuration" and combines neighboring electrodes forming adjacent pairs of electrodes [9]. Figure 2 illustrates the principle of rotating the locations of current injection (I) and voltage drop measurements (V) in this electrode configuration.

In the left figure, an alternating current I is injected at time t between electrodes 1 and 2 while corresponding voltages are sequentially measured at all remaining electrode pairs (e.g., $N - 3 = 13$ combinations). Afterwards, at time $t + \Delta T$ the location of current injection is rotated to the next pair of electrodes (electrodes 2 and 3, right figure) and again the corresponding voltages are sequentially measured at the remaining 13 electrode pairs. One image can be computed as soon as all electrode pairs have been used to inject current.

Temporal resolution may be relatively high in EIT (13–50 frames/s), with the potential to cover both ventilation and perfusion in real time. In contrast, spatial resolution of the images is significantly lower and at best limited to the distance between electrodes (ca. 2–3 cm).

Absolute and relative images

Obtaining accurate absolute EIT images is difficult because this requires detailed knowledge about geometry and absolute electrode positioning [11]. To circumvent this problem and improve the quality of EIT images, Barber [12] and later Hahn et al. [13] introduced the concept of "relative" EIT imaging. Here, the average impedance over a certain time window is subtracted from the actual impedance value which establishes a contrast amplification and cancels most of the geometric artifacts common in absolute EIT images. However, the price paid is the loss of absolute impedance information, i.e., only impedance changes ΔZ_n remain visible. Whereas the information on regional ventilation is preserved, a differential diagnosis of (non-ventilated) constant-impedance areas is not directly possible anymore (like distinguishing between overdistension, pneumothorax, excess in pleural fluid, or atelectasis).

A common way to visualize EIT images is to use a rainbow-color scheme [14], where red represents inspiration (highest relative impedance values), green codes for the breathing baseline, and blue (lowest relative impedance values) expiration. Figure 3 presents an example of the resulting colored image stream.

In a recent consensus paper [15], a different color scale was introduced where red implies low impedance (liquid) and azure stands for high impedance (air) with medium levels in black. Some of the commercial devices which became recently available use similar color schemes spanning from black to ultramarine blue-white for ventilation.

Functional imaging (fEIT)

The concept of functional EIT imaging was originally introduced in 1995 [13, 16]. Basically, this concept aims at imaging global and local ventilation activity over a certain period of time which can be selected by the user (e.g., 30 s).

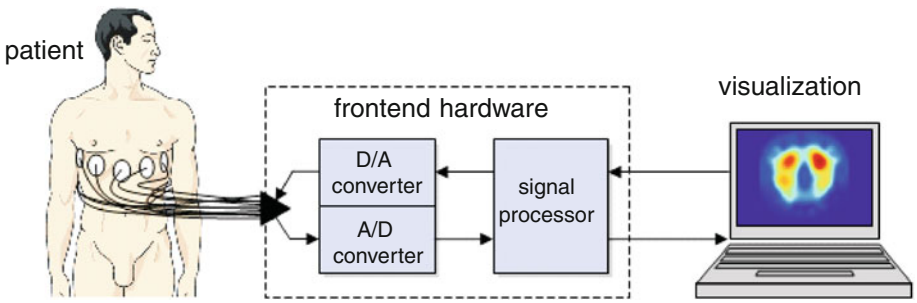

Fig. 1 EIT measurement scenario with electrodes equidistantly attached to the torso of the patient, and with some front-end and some visualization electronics

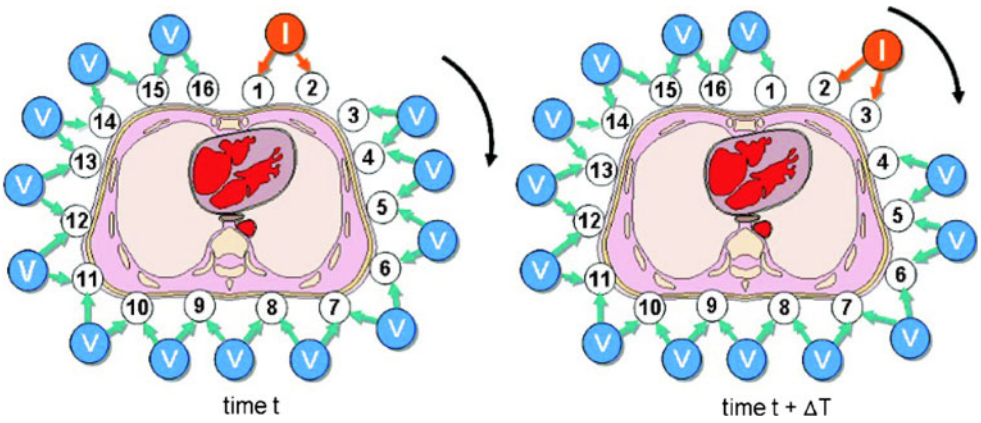

Fig. 2 $N = 16$ electrodes in an adjacent drive configuration. Within a few milliseconds, both the current electrodes and the active voltage electrodes are repeatedly rotated around the body. (Cross section of torso adopted from [10])

The authors proposed to quantify amplitudes of ventilation activity by computing local standard deviations at each pixel and plotting them at the corresponding image position. Such fEIT images (Fig. 4) provide a steady-state map of activity (mainly regional ventilation) causing impedance changes in the corresponding cross section of the body.

fEIT images are especially useful to position cursors and define regions of interest (ROIs), like specific pixels, layers, or quadrants. Furthermore, they allow one to study the ventilation distribution (e.g., regarding its homogeneity). Hence, positioning cursors at selected ROIs in fEIT images in combination with looking at the corresponding time courses of local impedance curves has facilitated the specific study of the ventilation distribution (Fig. 5). If selected properly, local impedance changes may not only display pulmonary but also cardiac-related impedance changes.

Techniques for ventilation monitoring

Relation between global and regional ventilation

As mentioned above, fEIT images are thought to capture and image local ventilation activity. Hence, summing up all pixels displayed in an fEIT image is referred to as global ventilation activity (GVA). A similar index named global tidal variation may be computed by summing all local ventilation-induced impedance changes $\Delta Z_{\text{local,max}} - \Delta Z_{\text{local,min}}$.

The correlation of global ventilation with global impedance measurements ΔZ_{global} resulting from EIT image streams has been investigated by many researchers, e.g., using a large syringe for a predefined gas or fluid volume injection (air, albumin solution) into the lungs [18], and using plethysmography [19].

An interesting question is whether changes in end-expiratory lung impedance (EELI) correlate with changes in end-expiratory lung volume (EELV). In dogs, a linear increase in impedance was demonstrated when the lung was inflated with a calibrated syringe [18]. Similarly, using multi-breath nitrogen washout as a reference, a good correlation ($R^2 = 0.95$) between ΔEELI and ΔEELV was found in a small human positive end-expiratory pressure (PEEP) trial involving 10 patients [20]. Using a super syringe as a reference, this question was also investigated in a lavage model involving 14 pigs [21]. In this trial, the authors quantified changes in regional functional residual capacity (FRC) based on local

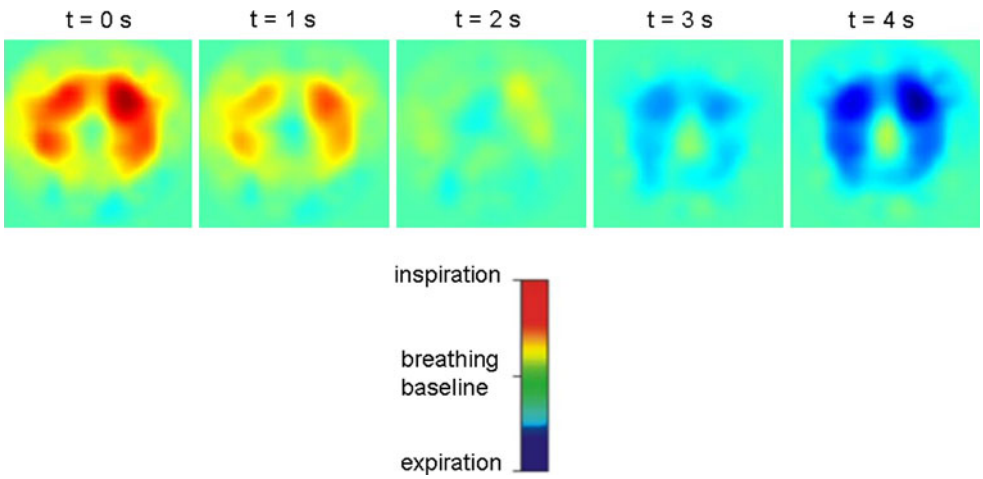

Fig. 3 Sequence of a rainbow-colored resting breathing cycle using relative EIT images based on ΔZ_n, according to [13]

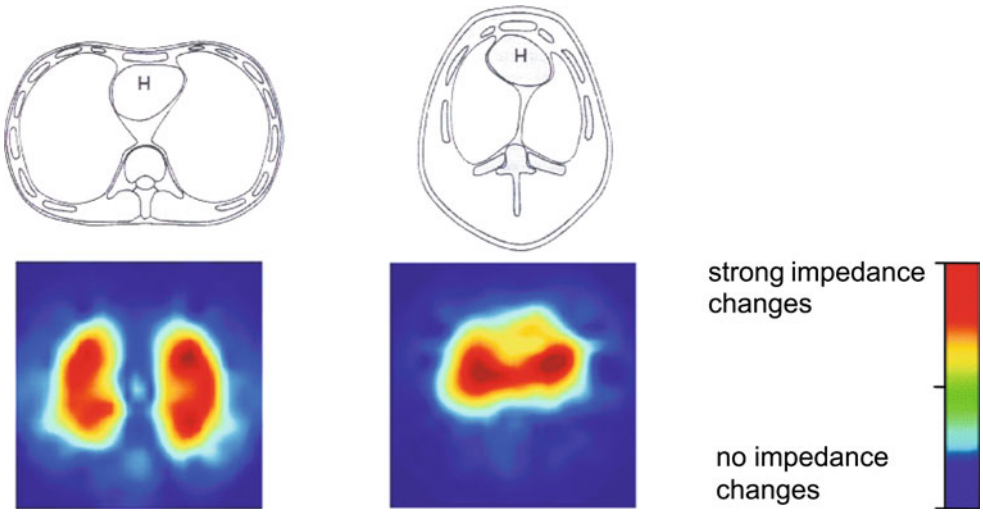

Fig. 4 Differences in geometry and corresponding rainbow-colored fEIT images of a human (*left*) and a pig (*right*). Strong impedance in *red* indicates regions of ventilatory activity, whereas low impedance changes (*blue*) point at no regional ventilation. Note the different meaning of the color scheme as compared to Fig. 3. Modified from [17]

ΔEELI in four different layers and reported a good correlation between (global) EELV and EELI ($R^2 > 0.95$). In a clinical study including 12 patients, a correlation of $R^2 = 0.92$ between changes in EELI and spirometric measurements of tidal volume was demonstrated [22]. For illustration, Fig. 6 shows the time course of global impedance ΔZ_{global} during a recruitment maneuver.

However, the results presented by Bikker et al. [23] from a human trial including 25 ARDS patients only showed a moderate correlation and therefore do not support the assumption of a purely linear relationship between global ΔEELI and ΔEELV. This weaker correlation may be based on severe changes in lung geometry due to heterogeneously impaired lung regions (atelectasis, overdistension, normally aerated regions). On the other hand, the conclusion of this study may be somewhat misleading as the chosen belt position (7th intercostal space) might be low enough for the diaphragm to enter the measurement field for low PEEPs. This could explain the low correlation. Thus, the overwhelming scientific information today is that ΔEELI can be scaled and converted to volume (ml) by using the global tidal variation, accepting that changes in intrathoracic blood volume occur when changing PEEP and this must be corrected for by taking into account the global tidal variation at the different PEEP levels.

In 2002, the correlation between regional ventilation and electron-beam computed tomography (EBCT) was studied in six pigs [24]. A good correlation ($R = 0.81$–0.93 depending on the lung region) between EIT and EBCT measurements was reported. Shortly after, similar findings were presented in a human study of 10 patients during slow inflation maneuvers [25], with a correlation of $R^2 = 0.96$ between regional air content changes determined by CT and impedance changes measured by EIT. Other studies validating regional EIT information include dynamic X-ray computed tomography (CT) in pigs [26], single-photon emission computed tomography (SPECT) [27], and positron emission tomography (PET) [28]. In conclusion, at present most researchers no longer question the fact that EIT correlates well with regional ventilation in the torso.

ΔfEIT imaging

The concept of ΔfEIT imaging was introduced in [29] and [30]. Basically, an fEIT image representing a specific situation at time t_2 is compared to an fEIT image at a previous time t_1 and the changes are contrast-amplified by a pixel-by-pixel subtraction. In order to obtain an approximation for changes in regional tidal volume, the difference is normalized by tidal volume V_T divided by GVA (Fig. 7).

It is anticipated that this specific technique provides clinically important information on regional gain or loss of ventilation when changing ventilator settings. For example, to find an optimal PEEP in a decremental PEEP trial, global information like the tidal volume may be misleading. As shown in Fig. 7, global tidal variation still increased while reducing PEEP from 15 to 10 cm H_2O already caused a significant loss in dorsal ventilation, but was superimposed by a larger gain in ventral ventilation. Although the following statement remains debatable [31], it is widely accepted that a very inhomogeneous ventilation would not be beneficial for severely sick patients, but will increase the risk of ventilator-induced lung injury (VILI).

Recently, ΔfEIT imaging was successfully applied within a small human patient trial [32].

Derived indices

Although EIT images and movies match well with the visual system of human operators, it is rather difficult to quantify information based on EIT image data. Since quantification is a prerequisite for therapeutic decisions,

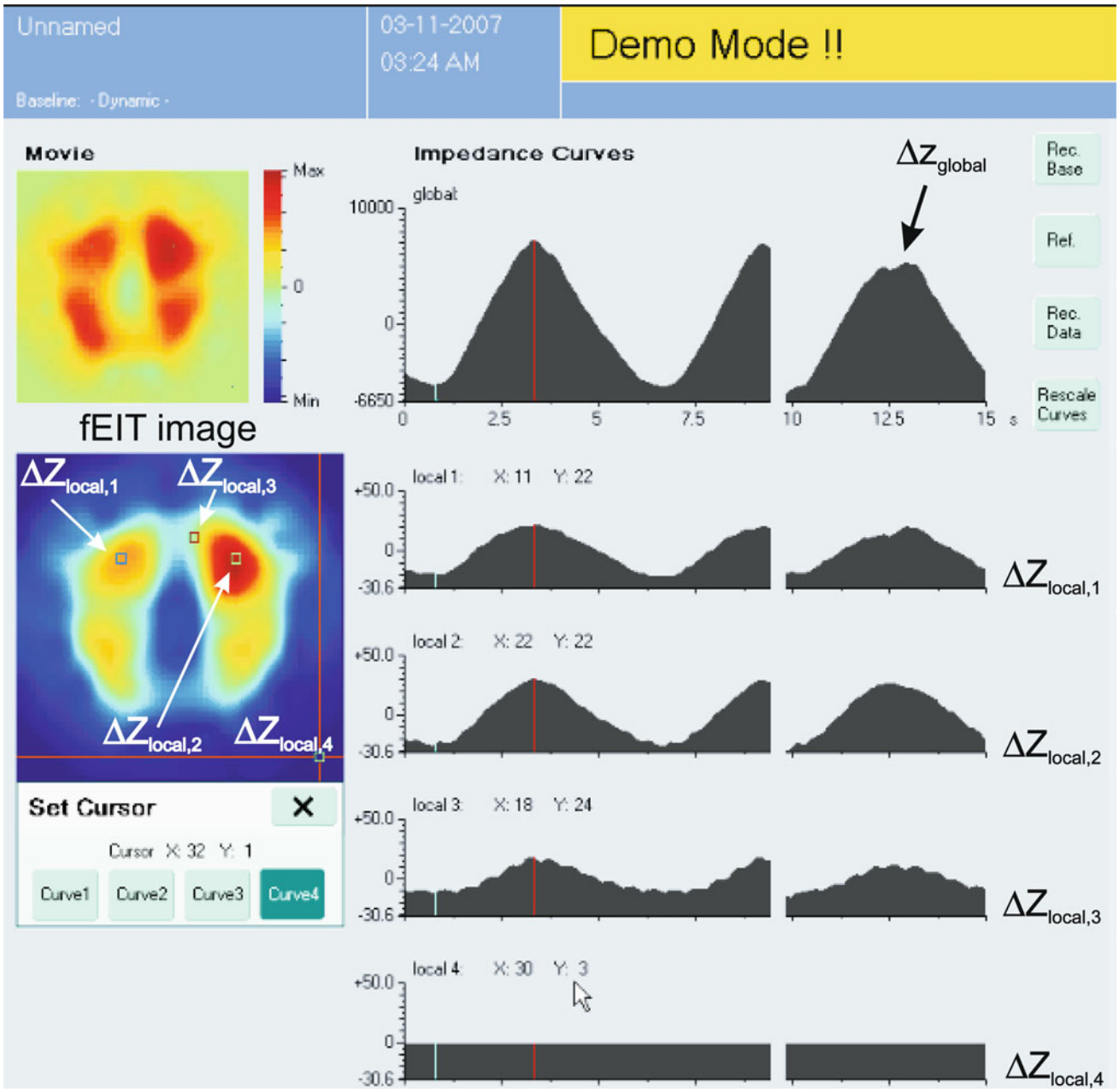

Fig. 5 Example of global and local impedance time courses (*right curves*) in a human subject. While the image stream of relative EIT frames is displayed as a movie (*upper left corner*), the fEIT image may conveniently be used for positioning cursors on selected ROIs. Note that in this example, $\Delta Z_{local,3}$ shows cardiac activity superposed on the ventilatory signal, whereas $\Delta Z_{local,4}$ positioned in the lower right corner shows no ventilatory activity at all

the following section reviews the literature regarding established numerical indices for EIT images.

Impedance ratio

In the year 2000, a new index called the impedance ratio (IR) was introduced which divided the ventilation activity in the upper (ventral) region $VA_{ventral}$ of fEIT images by the dorsal ventilation activity VA_{dorsal} [33]. This index turned out to be a sensitive parameter for following recruitment and derecruitment in animal trials.

Center of ventilation

The idea of using the center of gravity (CoG) as an index to characterize the shape of functional EIT images was

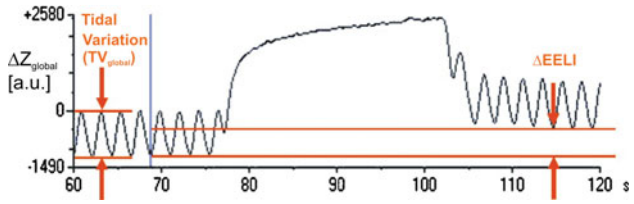

Fig. 6 Time course of global impedance ΔZ_{global} showing the effect of a 40-s recruitment maneuver

originally introduced in [34]. Considering the application, this index was named center of ventilation (CoV). This concept can be extended to characterize shapes of fEIT images as well. In 2007, it was demonstrated that y_{cog} may serve as a sensitive index to describe vertical shifts in ventilation due to opening and closing of the lung during incremental and decremental PEEP trials [28].

Regional delay index

The concept of imaging regional delays in ventilation during slow inflation maneuvers was introduced in [26]. Basically, the so-called regional ventilation delay (RVD) index quantifies the delay time needed for the regional impedance–time curve to reach a certain threshold of the maximal local impedance. Hence, it quantifies not just regional, but also temporal information from the EIT images, mainly on cyclic opening and closing. Recently, this concept was extended by providing maps of RVD standard deviations which correlate well with lung inhomogeneity [4, 35].

Homogeneity index

Another simple index called the global inhomogeneity index (GI) was proposed in [36, 37]. To calculate the GI, one has to compute the median value of regional impedance changes from the tidal image, then calculate the sum of differences between the median and every pixel value, and finally normalize by the sum of impedance values within the lung area. As reported, this index was able to differentiate ventilation inhomogeneity during one-lung ventilation. The performance of this index was investigated on a total of 50 patients [36], out of which 40 patients were tracheally intubated with double-lumen tubes (test group) and 10 patients serving as a control group were under anesthesia without pulmonary disease. One-lung ventilation was clearly distinguishable from double-lung ventilation for all patients. Furthermore, the GI index was found to be usable for PEEP titration in a pig trial where it correlated well with maximum compliance [37].

Quantification of regional overdistension and atelectasis

Another index which allows one to quantify regional overdistension and atelectasis was introduced in [38] and recently extended [39]. The methods assumes a uniform pressure distribution within the lung and introduces the concept of pixel compliance, i.e., $\Delta Z/(P_{plateau} - PEEP)$. By comparing the pixel compliance to the maximum regional compliance, an index for overdistension or atelectasis can be derived.

Application examples

Quantifying the effects of suctioning and disconnection

In an animal model and in a small clinical trial (13 ICU patients), it was recently demonstrated using EIT that functional residual capacity (FRC) is affected during bronchoscopic suctioning [40]. Also, the effects of disconnection and endotracheal suctioning in nine ventilated pigs were described [41]. Here, EIT was used to quantify the changes in regional compliance affecting mainly the dorsal lung regions.

In 2007, Wolf et al. [42] reported on using EIT to quantify the effect of derecruitment and suctioning in six children with acute lung injury (ALI). Similarly, a

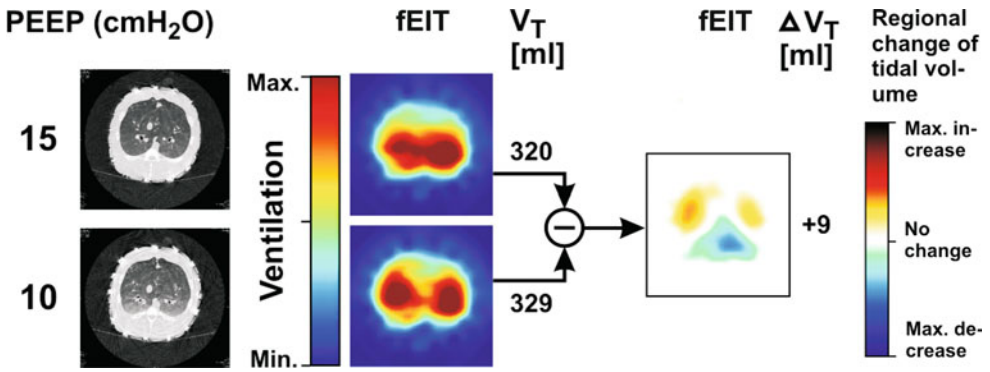

Fig. 7 Basic concept of ΔfEIT imaging, modified from [29]. In this example, PEEP has been reduced from 15 to 10 cm H_2O. While global V_T increased from 320 to 329 ml, dorsal atelectasis developed and the distribution of ventilation became much more inhomogeneous indicating that this PEEP was already too low. Note that the two *color codes* have different meanings

substantial loss of lung volume during endotracheal suctioning and the dynamics of recovery were demonstrated by Tingay et al. [43] in six 2-week-old piglets and by van Veenendaal et al. [44] in 12 preterm infants.

Unilateral intubation and placement of endotracheal tube

As reported in [45], EIT may be useful to position a tracheal tube. In a study of 40 patients, double-lumen tubes were employed to establish selective one-lung ventilation for thoracic surgery. Fibre-optic bronchoscopy was used to confirm double-lumen tube position. It was concluded that EIT allows the accurate online display of left and right lung ventilation and enables the clinician to check the proper positioning of the tube.

Regional pressure–volume curves

It is well known that surfactant-depleted lungs develop a sigmoidal pressure–volume (*P*–*V*) curve characterized by a dedicated lower inflection point (LIP) and an upper inflection point (UIP) [46, 47]. Regional *P*–*V* curves using EIT were investigated in [48] and results from four horizontal layers of diseased animal lungs were presented. Here, the underlying assumption was that ventilation pressure is effective and constant throughout the lung. Furthermore, as introduced above, ΔZ_{local} was assumed to represent regional lung volume changes [24, 25]. The resulting opening pressures varied significantly in the different lung layers, with the highest pressures found in the dorsal lung layer. This work was extended by proposing to image the regional distribution of LIP and UIP in different parts of the lung [49, 50]. The regional differences of LIP and the homogenizing effect of high-frequency oscillatory ventilation (HFOV) on the distribution of regional *P*–*V* curves in ALI pigs were reported in [51]. In [52], the use of regional *P*–*V* loops and compliance for titrating PEEP was proposed and demonstrated in 16 neonatal piglets. Similarly, on the basis of the results of 16 ALI/ARDS patients, it was recently demonstrated that proper analysis of regional *P*–*V* loops and compliance may be useful to identify individual changes in gas distribution, lung recruitability, and help to individually select PEEP [53].

Pneumothorax monitoring

Although uncommon, a pneumothorax is a potentially dangerous incident that may arise unexpectedly. By definition, in such an incident air is released into the thoracic cavity. As demonstrated in 2008, EIT can be used to quickly detect the development of an artificial pneumothorax in a controlled experimental setting [54]. Shortly thereafter, the time course of an accidental pneumothorax which unexpectedly occurred during an open lung animal experiment was reported [55].

However, while detection of accidental pneumothorax certainly is an advantage, long-term pneumothorax monitoring using EIT may be impractical as there may be a chance of developing an ulcer and necrosis in dorsal regions due to electrode belt pressure.

Pulmonary edema

Few studies have investigated whether EIT can be used to quantify the amount of fluid volume in the lung. In 1999, it was investigated how the IR index compares to extravascular lung water (EVLW) determined by the thermal dye double indicator dilution technique (TDD) [56]. Fourteen ALI/ARDS patients were included into the study and a significant correlation between changes in EVLW as measured by TDD and EIT ($R = 0.85$; $p < 0.005$) was presented. Using an eight-electrode EIT device with reduced spatial resolution, a strong correlation between thoracic resistivity and removed pleural fluid in 11 pleural effusion (PE) patients was recently reported [57].

Recruitment and derecruitment

It is well known that gravity may cause dorsal atelectasis in diseased patients, while ventral regions may be normally ventilated and sometimes even overdistended. Hence, monitoring the transverse distribution of ventilation is an important application of EIT, especially as a function of PEEP.

For illustration, Fig. 8 demonstrates the shift of regional ventilation due to PEEP. In this animal, ALI was induced by repetitive lung lavage [58] with saline warmed to 37 °C.

Although some authors used the IR index to quantify shifts in ventilation [33, 59], it was shown in [29] that the center of gravity y_{cog} may be employed to quantify such shifts during incremental and decremental PEEP trials. Similarly, by counting active pixels, shifts of ventilation activity due to PEEP changes were quantified in eight patients [60]. Furthermore, it was recently proposed to use EIT for local compliance estimation leading to means to access lung recuitability [61]. In [62], it was pointed out that y_{cog} correlates well with oxygenating efficiency during high-frequency oscillatory ventilation.

On the basis of CT measurements in two patients, Costa et al. [38] introduced the concept of pixel compliance and presented an EIT-based technique to quantify alveolar collapse and regional overdistension based on these indices. Recently, Costa's technique was successfully applied during a stepwise recruitment maneuver in nine ALI/ARDS patients [39].

Perfusion monitoring

As the perfusion-related changes in thoracic impedance are about one order of magnitude smaller than the changes induced by ventilation, it is much more difficult to extract information on stroke volume (SV), cardiac output (CO or Q), or lung perfusion.

Examples of early work on this subject were published in 1996 [63]. These studies focussed on the determination of stroke volume in healthy volunteers and used magnetic resonance imaging (MRI) as a reference. As has been demonstrated for idiopathic pulmonary arterial hypertension (IPAH) [64, 65], there may be more important connections between ventilation and cardiac-related impedance signals, as these patients expressed significantly lower impedance changes in the cardiac frequency band as compared to healthy controls.

At present, all attempts to quantify perfusion are still in the research stage and not yet available at the bedside. Some algorithmic questions remain to be answered, for which some approaches will be reviewed in the following subsections. However, the potential is large, as EIT-based perfusion monitoring would allow one not only to image local perfusion but also to establish local ventilation/perfusion (V/Q) mappings.

Separation of cardiac- and ventilation-related EIT signals

This approach relies on the separation of the ventilation-related signal (VRS) and the cardiac-related signals (CRS) based on frequency content and was originally introduced in the early 1990s [66, 67]. It has been successfully employed in a bilateral ventilation study to quantify left-to-right lung perfusion ratios in 10 patients scheduled for elective chest surgery [68]. By employing such frequency-domain filtering techniques on EIT measurements, Carlisle et al. recently reported [69] gravity-dependent differences in the distribution of perfusion and ventilation were in 26 preterm infants.

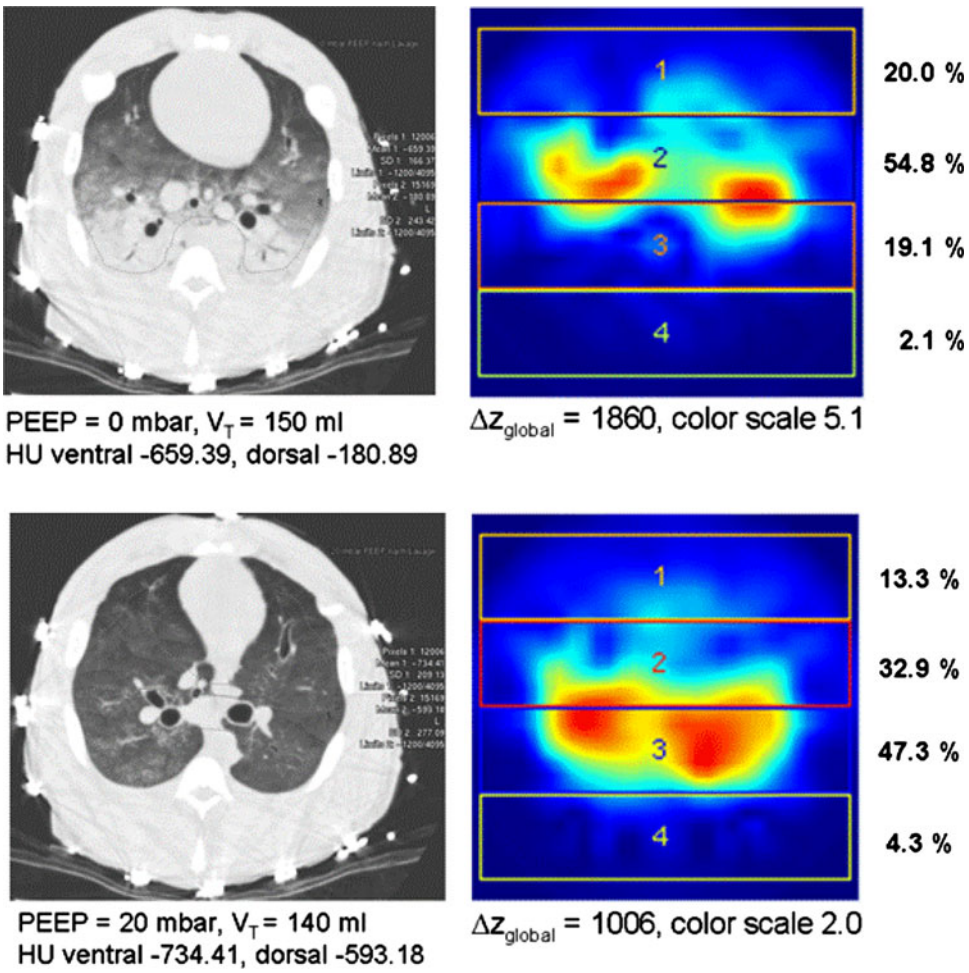

Fig. 8 CT scan and corresponding fEIT image with four layers in an ALI pig ventilated with FiO_2 50 %, I:E 1:1 and $\Delta p = 10$ mbar. *Upper images* (PEEP = 0 mbar): CT scan shows dorsal atelectasis. In the fEIT image, the main ventilation activity (54.8 % of all ventilation activity) occurs in layer 2. *Lower images* (PEEP = 20 mbar): main ventilation activity has shifted to layer 3 (47.3 %) of the fEIT image and ventilation is much more homogenous. At the same time, the corresponding CT scan shows no atelectasis anymore (data from the authors, not published)

ECG gating

This technique amplifies the CRS by assuming that it has a deterministic characteristic and that VRS is completely uncorrelated with CRS [70–73]. The QRS complex of the synchronously measured ECG signal is used as a trigger. By summing up the images over, e.g., 200 heart cycles starting at each QRS complex, the signal strength of CRS is selectively amplified by a factor of $\sqrt{200} \approx 14$ in comparison to the relative strength of VRS. Additional electrodes for ECG measurements may not be necessary, as the EIT electrodes themselves could be used. Note, however, that considering 200 heart cycles implies that a later visualization of CRS on screen would be delayed by $200/2 = 100$ heart beats, which excludes real-time analysis.

Apnea methods

In this approach, ventilation is briefly interrupted to quantify impedance changes introduced solely by heart activity (CRS). On the basis of this method, it was recently investigated whether EIT is capable of monitoring stroke volume and perfusion [74]. In this study, cardiac preload, and thus pulmonary perfusion, was reduced by inflating a balloon of a Fogarty catheter positioned in the inferior caval vein or by increasing the PEEP. Stroke volume (SV) was derived using a pulmonary artery catheter and thermodilution method. A reasonable beat-to-beat correlation between stroke volume and the EIT global impedance signal during apnea was found. Shortly thereafter, it was shown that measurements of global impedance during ventilation and during apnea could be used to produce regional Z_V/Z_Q values in distinct ROIs [75]. Despite remaining limitations, it was pointed out that such EIT measurements may have the potential to eventually produce local *V*/*Q* mappings. However, although inducing a short apnea for such measurements may not severely harm the patient, it changes the ventilatory situation. Hence, it is not guaranteed that the same perfusion will occur during ventilation and during apnea.

Use of contrast agents

As was demonstrated in [24], hypertonic saline solutions may be used as an electrical impedance contrast agent. In this work, a Swan–Ganz catheter was positioned in a pulmonary artery branch and 5.85 % saline solution was administered as a bolus. EBCT scans and a radiographic contrast material were used as a reference. The authors were able to track the high salt concentration bolus in three pigs on its way from the right heart via the lungs to the left heart. Similar findings using a 10 % hypertonic saline solution and SPECT measurements for reference in four pigs were reported in [76]. A similar scenario was recently described in [77]. Although these results are preliminary, this approach seems to have some potential for quantification and future clinical application, as most patients on the ICU have a central venous catheter in place. However, a principal limitation is that the analysis is not beat-to-beat and delayed by the time-of-flight necessary for the passage of the contrast agent (about 10 s).

Separation based on principal component analysis

In 2008, a new algorithm based on principal component analysis (PCA) was introduced [78]. For convenience, Fig. 9 provides an example of successful separation of CRS and VRS using PCA in a pig trial. Note the heart-related activity in the right image which is not visible in the ventilation image.

While being the first specific algorithm of its kind to separate the two signal components in a beat-to-beat mode, some of the underlying theoretical basis has already been presented in 2001 [79]. Provided there is enough computational power, this promising approach has the potential to be fast enough for beat-to-beat monitoring. For illustration, we provide another supplementary material 1 which is an example of successful CRS (right) and VRS (middle) separation from the raw image stream (left). However, at present the results are still preliminary and require confirmation in larger trials.

Outlook

For the transition of EIT from the research lab to the ICU, clinicians will require not only useful applications but also sufficient ease of handling. Important aspects of the user interface, such as electrode belts and ways to visually represent information on screen, will be key issues for this transition.

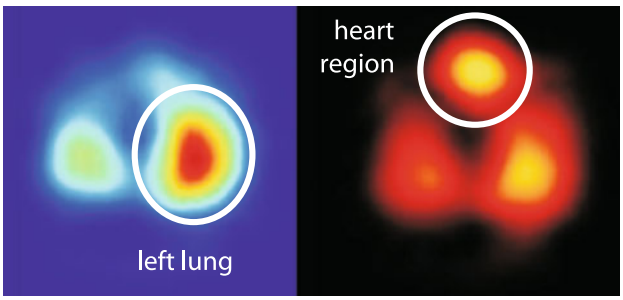

Fig. 9 Successful separation of an EIT image stream into a pulmonary-related EIT signal (*left, rainbow color scheme*) and an amplified cardiac-related EIT signal (*right, black-red-white coloring*) using PCA. The corresponding video is provided as electronic supplementary material 2

Especially with respect to the ALI/ARDS patient population, there is a strong need for consensus on hardware, color schemes, and imaging algorithms, like the one provided in [15], in order to be able to move on to multi-center trials while staying compatible.

Although regional ventilation will become the first clinical EIT target application, it is foreseeable that regional perfusion and regional *V/Q* mappings are next in line. However, other possible extensions of current planar monofrequent EIT include techniques like multifrequency tomography [80, 81] or three-dimensional impedance tomography [5, 82, 83]. Finally, while being a difficult algorithmic problem, absolute EIT (aEIT) imaging [84, 85] has the potential to differentiate between non-ventilated areas containing mainly pulmonary air (pneumothorax) or fluid (atelectasis, edema, pleural effusion). Eventually, aEIT may even allow one to quantify changes in FRC.

Conclusions

Electrical impedance tomography is a new monitoring modality that will change the way we treat patients by mechanical ventilation. It will allow us to tune and optimize regional ventilation of the individual patient which, until now, is difficult at the bedside. Furthermore, there is potential for future extensions, including regional perfusion monitoring, regional *V/Q* mapping and, possibly, quantifying pneumothorax, atelectasis, pulmonary edema, and possibly the onset of pneumonia at an early stage.

In 2004, Arnold anticipated that EIT would lead to the "holy grail of ventilation monitoring" [1]. On the basis of the evidence provided in this review, we believe that he was right, but possibly regional ventilation monitoring is just the dawn of a new era of opportunities.

Acknowledgments The authors thank Laraine Visser-Isles, Rotterdam, the Netherlands, for proofreading of the English manuscript. The authors gratefully acknowledge the permission to use the Dräger EIT Evaluation Kit 2 (EEK2) for unrestricted research into animals and human trials.

Conflicts of interest S. Leonhardt discloses financial support for unrestricted research into EIT-based perfusion imaging from Dräger Medical GmbH, Lübeck, Germany. He has also received honoraria for lecturing and consulting.

References

1. Arnold JH (2004) Electrical impedance tomography: on the path to the holy grail. Crit Care Med 32:894–895
2. Bodenstein M, David M, Markstaller K (2009) Principles of electrical impedance tomography and its clinical application. Crit Care Med 37:713–724
3. Costa EL, Lima RG, Amato MB (2009) Electrical impedance tomography. Curr Opin Crit Care 15:18–24
4. Muders T, Luepschen H, Putensen C (2010) Impedance tomography as a new monitoring technique. Curr Opin Crit Care 16:269–275
5. Moerer O, Hahn G, Quintel M (2011) Lung impedance measurements to monitor alveolar ventilation. Curr Opin Crit Care 17:260–267
6. Putensen C, Wrigge H, Zinserling J (2007) Electrical impedance tomography guided ventilation therapy. Curr Opin Crit Care 13:344–350
7. Domenighetti G, Maggiorini M (2010) Electrical impedance tomography to guide ventilation in ALI-ARDS patients: a research tool for zealous physiologists or an imminent support for the real world intensivist? Minerva Anestesiol 76:986–988
8. Frerichs I, Weiler N (2012) Electrical impedance tomography: the next game level. Crit Care Med 40:1015–1016
9. Avis NJ, Barber DC (1994) Image reconstruction using non-adjacent drive configurations. Physiol Meas 15(Suppl 2a):153–160
10. Malmivuo J, Plonsey R (1995) Bioelectromagnetism—principles and applications of bioelectric and biomagnetic fields. Oxford University Press, New York
11. Brown BH (2003) Electrical impedance tomography (EIT): a review. J Med Eng Technol 27:97–108
12. Barber DC (1990) Quantification in impedance imaging. Clin Phys Physiol Meas 11:45–56
13. Hahn G, Sipinkov I, Baisch F, Hellige G (1995) Changes in the thoracic impedance distribution under different ventilatory conditions. Physiol Meas 16:161–173
14. Calzia E, Hahn G, Hellige G (2005) Electrical impedance tomography: looking behind the secrets of regional lung function. Intensive Care Med 31:1474–1475
15. Adler A, Arnold JH, Bayford R, Borsic A, Brown B, Dixon P, Faes TJ, Frerichs I, Gagnon H, Gärber Y, Grychtol B, Hahn G, Lionheart WR, Malik A, Patterson RP, Stocks J, Tizzard A, Weiler N, Wolf GK (2009) GREIT: a unified approach to 2D linear EIT reconstruction of lung images. Physiol Meas 30:S35–S55
16. Frerichs I, Hahn G, Hellige G (1999) Thoracic electrical impedance tomographic measurements during volume controlled ventilation—effects of tidal volume and positive end-expiratory pressure. IEEE Trans Med Imaging 18:764–773
17. Meier T, Leibecke T, Eckmann C, Gosch UW, Grossherr M, Bruch HP, Gehring H, Leonhardt S (2006) Electrical impedance tomography: changes in distribution of pulmonary ventilation during laparoscopic surgery in a porcine model. Langenbecks Arch Surg 391:383–389
18. Adler A, Amyot R, Guardo R, Bates JH, Berthiaume Y (1997) Monitoring changes in lung air and liquid volumes with electrical impedance tomography. J Appl Physiol 83:1762–1767

19. Marquis F, Coulombe N, Costa R, Gagnon H, Guardo R, Skrobik Y (2006) Electrical impedance tomography's correlation to lung volume is not influenced by anthropometric parameters. J Clin Monit Comput 20:201–207
20. Hinz J, Hahn G, Neumann P, Sydow M, Mohrenweiser P, Hellige G, Burchardi H (2003) End-expiratory lung impedance change enables bedside monitoring of end-expiratory lung volume change. Intensive Care Med 29:37–43
21. Odenstedt H, Lindgren S, Olegrd C, Erlandsson K, Lethvall S, Aneman A, Stenqvist O, Lundin S (2005) Slow moderate pressure recruitment maneuver minimizes negative circulatory and lung mechanic side effects: evaluation of recruitment maneuvers using electric impedance tomography. Intensive Care Med 31:1706–1714
22. Grivans C, Lundin S, Stenqvist O, Lindgren S (2011) Positive end-expiratory pressure-induced changes in end-expiratory lung volume measured by spirometry and electric impedance tomography. Acta Anaesthesiol Scand 55:1068–1077
23. Bikker IG, Leonhardt S, Bakker J, Gommers D (2009) Lung volume calculated from electrical impedance tomography in ICU patients at different PEEP levels. Intensive Care Med 35:1362–1367
24. Frerichs I, Hinz J, Herrmann P, Weisser G, Hahn G, Quintel M, Hellige G (2002) Regional lung perfusion as determined by electrical impedance tomography in comparison with electron beam CT imaging. IEEE Trans Med Imaging 21:646–652
25. Victorino JA, Borges JB, Okamoto VN, Matos GF, Tucci MR, Caramez MP, Tanaka H, Sipmann FS, Santos DC, Barbas CS, Carvalho CR, Amato MB (2004) Imbalances in regional lung ventilation: a validation study on electrical impedance tomography. Am J Respir Crit Care Med 169:791–800
26. Wrigge H, Zinserling J, Muders T, Varelmann D, Gnther U, von der Groeben C, Magnusson A, Hedenstierna G, Putensen C (2008) Electrical impedance tomography compared with thoracic computed tomography during a slow inflation maneuver in experimental models of lung injury. Crit Care Med 36:903–909
27. Hinz J, Neumann P, Dudykevych T, Andersson LG, Wrigge H, Burchardi H, Hedenstierna G (2003) Regional ventilation by electrical impedance tomography: a comparison with ventilation scintigraphy in pigs. Chest 124:314–322
28. Richard JC, Pouzot C, Gros A, Tourevieille C, Lebars D, Lavenne F, Frerichs I, Gurin C (2009) Electrical impedance tomography compared to positron emission tomography for the measurement of regional lung ventilation: an experimental study. Crit Care 13:R82
29. Luepschen H, Meier T, Grossherr M, Leibecke T, Karsten J, Leonhardt S (2007) Protective ventilation using electrical impedance tomography. Physiol Meas 28:247–260
30. Meier T, Luepschen H, Karsten J, Leibecke T, Grossherr M, Gehring H, Leonhardt S (2008) Assessment of regional lung recruitment and derecruitment during a PEEP trial based on electrical impedance tomography. Intensive Care Med 34:543–550
31. Costa EL, Amato MB (2010) Can heterogeneity in ventilation be good? Crit Care 14:134
32. Bikker IG, Leonhardt S, Reis Miranda D, Bakker J, Gommers D (2010) Bedside measurement of changes in lung impedance to monitor alveolar ventilation in dependent and non-dependent parts by electrical impedance tomography during a positive end-expiratory pressure trial in mechanically ventilated intensive care unit patients. Crit Care 14:R100
33. Kunst PW, Vazquez de Anda G, Bhm SH, Faes TJ, Lachmann B, Postmus PE, de Vries PM (2000) Monitoring of recruitment and derecruitment by electrical impedance tomography in a model of acute lung injury. Crit Care Med 28:3891–3895
34. Frerichs I, Hahn G, Golisch W, Kurpitz M, Burchardi H, Hellige G (1998) Monitoring perioperative changes in distribution of pulmonary ventilation by functional electrical impedance tomography. Acta Anaesthesiol Scand 42:721–726
35. Muders T, Luepschen H, Zinserling J, Greschus S, Fimmers R, Guenther U, Buchwald M, Grigutsch D, Leonhardt S, Putensen C, Wrigge H (2012) Tidal recruitment assessed by electrical impedance tomography and computed tomography in a porcine model of lung injury. Crit Care Med 40:903–911
36. Zhao Z, Moller K, Steinmann D, Frerichs I, Guttmann J (2009) Evaluation of an electrical impedance tomography-based global inhomogeneity index for pulmonary ventilation distribution. Intensive Care Med 35:1900–1906
37. Zhao Z, Steinmann D, Frerichs I, Guttmann J, Moller K (2010) PEEP titration guided by ventilation homogeneity: a feasibility study using electrical impedance tomography. Crit Care 14:R8
38. Costa EL, Borges JB, Melo A, Suarez-Sipmann F, Toufen C Jr, Bohm SH, Amato MB (2009) Bedside estimation of recruitable alveolar collapse and hyper-distension by electrical impedance tomography. Intensive Care Med 35:1132–1137
39. Gómez-Laberge C, Arnold JH, Wolf GK (2012) A unified approach for EIT imaging of regional overdistension and atelectasis in acute lung injury. IEEE Trans Med Imaging 31:834–842
40. Lindgren S, Odenstedt H, Erlandsson K, Grivans C, Lundin S, Stenqvist O (2008) Bronchoscopic suctioning may cause lung collapse: a lung model and clinical evaluation. Acta Anaesthesiol Scand 52:209–218
41. Lindgren S, Odenstedt H, Olegrd C, Sondergaard S, Lundin S, Stenqvist O (2007) Regional lung derecruitment after endotracheal suction during volume- or pressure-controlled ventilation: a study using electric impedance tomography. Intensive Care Med 33:172–180
42. Wolf GK, Grychtol B, Frerichs I, van Genderingen HR, Zurakowski D, Thompson JE, Arnold JH (2007) Regional lung volume changes in children with acute respiratory distress syndrome during a derecruitment maneuver. Crit Care Med 35:1972–1978
43. Tingay DG, Copnell B, Grant CA, Dargaville PA, Dunster KR, Schibler A (2010) The effect of endotracheal suction on regional tidal ventilation and end-expiratory lung volume. Intensive Care Med 36:888–896
44. van Veenendaal MB, Miedema M, de Jongh FH, van der Lee JH, Frerichs I, van Kaam AH (2009) Effect of closed endotracheal suction in high frequency ventilated premature infants measured with electrical impedance tomography. Intensive Care Med 35:2130–2134
45. Steinmann D, Stahl CA, Minner J, Schumann S, Loop T, Kirschbaum A, Priebe HJ, Guttmann J (2008) Electrical impedance tomography to confirm correct placement of double-lumen tube: a feasibility study. Br J Anaesth 101:411–418
46. Gattinoni L, Pesenti A, Avalli L, Rossi F, Bombino M (1987) Pressure-volume curve of total respiratory system in acute respiratory failure. Computed tomographic scan study. Am Rev Respir Dis 136:730–736
47. Pelosi P, D'Andrea L, Vitale G, Pesenti A, Gattinoni L (1994) Vertical gradient of regional lung inflation in adult respiratory distress syndrome. Am J Respir Crit Care Med 149:8–13

48. Kunst PW, Bohm SH, Vazquez de Anda G, Amato MB, Lachmann B, Postmus PE, de Vries PM (2000) Regional pressure volume curves by electrical impedance tomography in a model of acute lung injury. Crit Care Med 28:178–183
49. Hinz J, Moerer O, Neumann P, Dudykevych T, Frerichs I, Hellige G, Quintel M (2006) Regional pulmonary pressure volume curves in mechanically ventilated patients with acute respiratory failure measured by electrical impedance tomography. Acta Anaesthesiol Scand 50:331–339
50. Grychtol B, Wolf GK, Arnold JH (2009) Differences in regional pulmonary pressure impedance curves before and after lung injury assessed with a novel algorithm. Physiol Meas 30:137–148
51. van Genderingen HR, van Vught AJ, Jansen JR (2004) Regional lung volume during high-frequency oscillatory ventilation by electrical impedance tomography. Crit Care Med 32:787–794
52. Dargaville PA, Rimensberger PC, Frerichs I (2010) Regional tidal ventilation and compliance during a stepwise vital capacity manoeuvre. Intensive Care Med 36:1953–1961
53. Lowhagen K, Lundin S, Stenqvist O (2011) Regional intratidal gas distribution in acute lung injury and acute respiratory distress syndrome—assessed by electric impedance tomography. Minerva Anestesiol 76:1024–1035
54. Costa EL, Chaves CN, Gomes S, Beraldo MA, Volpe MS, Tucci MR, Schettino IA, Bohm SH, Carvalho CR, Tanaka H, Lima RG, Amato MB (2008) Real-time detection of pneumothorax using electrical impedance tomography. Crit Care Med 36:1230–1238
55. Preis C, Luepschen H, Leonhardt S, Gommers D (2009) Experimental case report: development of a pneumothorax monitored by electrical impedance tomography. Clin Physiol Funct Imaging 29:159–162
56. Kunst PW, Vonk Noordegraaf A, Raaijmakers E, Bakker J, Groeneveld AB, Postmus PE, de Vries PM (1999) Electrical impedance tomography in the assessment of extravascular lung water in noncardiogenic acute respiratory failure. Chest 116:1695–1702
57. Arad M, Zlochiver S, Davidson T, Shoenfeld Y, Adunsky A, Abboud S (2009) The detection of pleural effusion using a parametric EIT technique. Physiol Meas 30:421–428
58. Lachmann B, Robertson B, Vogel J (1980) In vivo lung lavage as an experimental model of the respiratory distress syndrome. Acta Anaesthesiol Scand 24:231–236
59. Kunst PW, de Vries PM, Postmus PE, Bakker J (1999) Evaluation of electrical impedance tomography in the measurement of PEEP-induced changes in lung volume. Chest 115:1102–1106
60. Hinz J, Moerer O, Neumann P, Dudykevych T, Hellige G, Quintel M (2005) Effect of positive end-expiratory-pressure on regional ventilation in patients with acute lung injury evaluated by electrical impedance tomography. Eur J Anaesthesiol 22:817–825
61. Lowhagen K, Lindgren S, Odenstedt H, Stenqvist O, Lundin S (2011) A new nonradiological method to assess potential lung recruitability: a pilot study in ALI patients. Acta Anaesthesiol Scand 55:165–174
62. Wolf GK, Grychtol B, Frerichs I, Zurakowski D, Arnold JH (2010) Regional lung volume changes during high-frequency oscillatory ventilation. Pediatr Crit Care Med 11:610–615
63. Vonk Noordegraaf A, Faes TJ, Marcus JT, Janse A, Heethaar RM, Postmus PE, de Vries PM (1996) Improvement of cardiac imaging in electrical impedance tomography by means of a new electrode configuration. Physiol Meas 17:179–188
64. Smit HJ, Vonk Noordegraaf A, Marcus JT, Boonstra A, de Vries PM, Postmus PE (2004) Determinants of pulmonary perfusion measured by electrical impedance tomography. Eur J Appl Physiol 92:45–49
65. Smit HJ, Vonk-Noordegraaf A, Boonstra A, de Vries PM, Postmus PE (2006) Assessment of the pulmonary volume pulse in idiopathic pulmonary arterial hypertension by means of electrical impedance tomography. Respiration 73:597–602
66. Zadehkoochak M, Blott BH, Hames TK, George RF (1992) Pulmonary perfusion and ventricular ejection imaging by frequency domain filtering of EIT images. Clin Phys Meas 13:191–196
67. Leathard AD, Brown BH, Campbell J, Zhang F, Morice AH, Tayler D (1994) A comparison of ventilatory and cardiac related changes in EIT images of normal human lungs and of lungs with pulmonary emboli. Physiol Meas 15:137–146
68. Frerichs I, Pulletz S, Elke G, Reifferscheid F, Schadler D, Scholz J, Weiler N (2009) Assessment of changes in distribution of lung perfusion by electrical impedance tomography. Respiration 77:282–291
69. Carlisle HR, Armstrong RK, Davis PG, Schibler A, Frerichs I, Tingay DG (2010) Regional distribution of blood volume within the preterm infant thorax during synchronised mechanical ventilation. Intensive Care Med 36:2101–2108
70. Eyueboglu B, Brown B (1988) Methods of cardiac gating applied potential tomography. Clin Phys Meas 9:43–48
71. Vonk Noordegraaf A, Kunst PW, Janse A, Marcus JT, Postmus PE, Faes TJ, de Vries PM (1998) Pulmonary perfusion measured by means of electrical impedance tomography. Physiol Meas 19:263–273
72. Smit HJ, Handoko ML, Vonk Noordegraaf A, Faes TJ, Postmus PE, de Vries PM, Boonstra A (2003) Electrical impedance tomography to measure pulmonary perfusion: is the reproducibility high enough for clinical practice? Physiol Meas 24:491–499
73. Vonk-Noordegraaf A, van Wolferen SA, Marcus JT, Boonstra A, Postmus PE, Peeters JW, Peacock AJ (2005) Noninvasive assessment and monitoring of pulmonary circulation. Europ Respir J 25:758–766
74. Fagerberg A, Stenqvist O, Aneman A (2009) Monitoring pulmonary perfusion by electrical impedance tomography: an evaluation in a pig model. Acta Anaesthesiol Scand 53:152–158
75. Fagerberg A, Stenqvist O, Aneman A (2009) Electrical impedance tomography applied to assess matching of pulmonary ventilation and perfusion in a porcine experimental model. Crit Care 13:R34
76. Luepschen H, Muders T, Pikkemaat R, Meier T, Putensen C, Leonhardt S (2010) Bestimmung der Lungenperfusion mittels Elektrischer Impedanztomographie. Rostock, Germany, pp 5–8 (in German)
77. Borges JB, Suarez-Sipmann F, Bohm SH, Tusman G, Melo A, Maripuu E, Sandstrom M, Park M, Costa EL, Hedenstierna G, Amato M (2012) Regional lung perfusion estimated by electrical impedance tomography in a piglet model of lung collapse. J Appl Physiol 112:225–236
78. Deibele J, Luepschen H, Leonhardt S (2008) Dynamic separation of pulmonary and cardiac changes in electrical impedance tomography. Physiol Meas 29:1–14
79. Kerrouche N, McLeod C, Lionheart W (2001) Time series of EIT chest images using singular value decomposition and Fourier transform. Physiol Meas 22:147–157

80. Li J (2000) Multifrequente Impedanztomographie zur Darstellung der elektrischen Impedanzverteilung im menschlichen Thorax. Dissertation, University of Stuttgart, Germany (in German)
81. Hahn G, Thiel F, Dudykevych T, Frerichs I, Gersing E, Schroder T, Hartung C, Hellige G (2001) Quantitative evaluation of the performance of different electrical tomography devices. Biomed Tech 46:91–95
82. Metherall P, Barber DC, Smallwood RH, Brown BH (1996) Three dimensional electrical impedance tomography. Nature 380:509–512
83. Bikker IG, Preis C, Egal M, Bakker J, Gommers D (2011) Electrical impedance tomography measured at two thoracic levels can visualize the ventilation distribution changes at the bedside during a decremental positive end-expiratory lung pressure trial. Crit Care 15:R193
84. Hahn G, Just A, Dudykevych T, Frerichs I, Hinz J, Quintel M, Hellige G (2006) Imaging pathologic pulmonary air and fluid accumulation by functional and absolute EIT. Physiol Meas 27:187–198
85. Denai MA, Mahfouf M, Mohamad-Samuri S, Panoutsos G, Brown BH, Mills GH (2010) Absolute electrical impedance tomography (aEIT) guided ventilation therapy in critical care patients: simulations and future trends. IEEE Trans Inf Technol Biomed 14:641–649